Available on CMS information server

CMS NOTE 2006/147

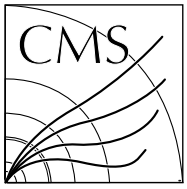

The Compact Muon Solenoid Experiment

CMS Note

Mailing address: CMS CERN, CH-1211 GENEVA 23, Switzerland

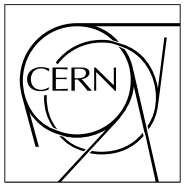

Simulation of Energy Response Linearity, Resolution and e^-/π Ratio for the CASTOR Calorimeter at CMS

P. Katsas, A. D. Panagiotou

University of Athens, Physics Department, Nuclear & Particle Physics Division

A. Zhokin

ITEP, Moscow, Russia

Abstract

The response linearity, the energy resolution and the e^-/π ratio for the CMS CASTOR calorimeter is studied using gammas, electrons and pions in the energy range of 20 - 1000 GeV. CASTOR is going to be installed in the very forward region of the CMS experiment.

1 Introduction

The CASTOR (Centauro And STrange Object Research) detector[1] is a quartz-tungsten sampling calorimeter proposed to study the very forward rapidity region in heavy ion collisions in the multi-TeV range at the LHC [3] and thus to complement the heavy ion physics programme, developed essentially in the baryon-free midrapidity region. The calorimeter is specialized in the detection and identification of potential "Centauros" and "Strangelets". CASTOR will be installed in the CMS experiment at 14.38 m from the interaction point, covering the pseudo-rapidity range $5.2 < \eta < 6.6$ and will, thus, contribute not only to the heavy ion program, but also to diffractive and low-x physics in pp collisions. The CMS and TOTEM detectors supplemented by the CASTOR calorimeter will constitute the largest acceptance system ever built at a hadron collider, having the possibility to measure the forward energy and particle flow up to $\eta = 6.6$.

2 Design of the calorimeter

The CASTOR detector is a Cherenkov-effect based calorimeter with tungsten (W) absorber and quartz (Q) as sensitive material. An incident high-energy particle will shower in the tungsten volume and produce relativistic charged particles that will emit Cherenkov light in the quartz plates. The absorber and quartz plates are inclined at 45^o with respect to the impinging particles, in order to maximize the Cherenkov light production. The calorimeter in the present MC study is azimuthally divided into 16 sectors ($\phi = 22.5^o$) and longitudinally segmented into 18 readout units (RU), see Figure 1. The electromagnetic part of the calorimeter consists of the first 2 RUs.

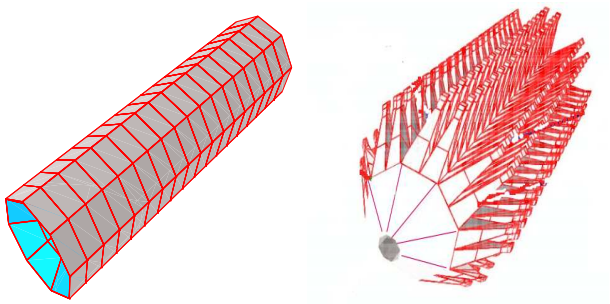

Figure 1: CASTOR's geometry. *Left:* View of the calorimeter's longitudinal segmentation. *Right:* View of the azimuthal segmentation and light guides.

The signal of the detector is Cherenkov light, which is collected and transmitted to light-reading devices through air-core light-guides. Figures 2, 3, show the longitudinal and azimuthal profile of the Cherenkov light produced by incoming electrons and pions respectively. CASTOR's longitudinal segmentation, with appropriate sampling steps, permits the reading of Cherenkov photons along the depth of the calorimeter, so that the energy deposited in each readout unit is measured. Figures 4a, b show the number of cherenkov photons collected per reading unit. This detailed information is necessary, in order to be able to identify potential highly penetrating objects, beyond the range of normal hadrons, producing long range signals in central Pb+Pb collisions. Highly penetrating components have been observed in hadron-rich (Centauro-type) events in high energy cosmic-ray interactions. The energy deposition pattern through the calorimeter, has been proposed as a signature of different kind of stable or unstable strangelets [2].

3 Simulation of the CASTOR calorimeter performance

The detector's specifications for this full simulation study within OSCAR are:

- Tungsten absorber plates of 5mm thickness.
- Quartz plates of 2mm thickness.
- Filling ratio of 40%.
- Each reading unit consists of 7 tungsten/quartz pairs, sampling units (SU) and corresponds to $20X_0$.
- Impact point arbitrarily chosen in the centre of one sector.
- Incident particles are electrons, gammas and pions in the energy range 20 - 1000GeV.

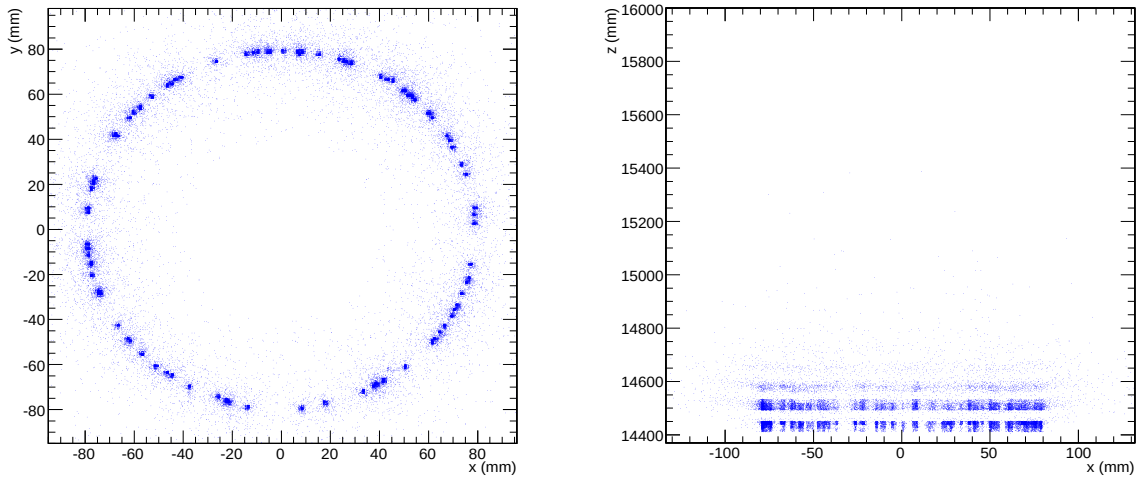

Figure 2: Cherenkov light yield transversal and longitudinal profile, produced by incoming 50GeV electrons. The particles enter at the center of the calorimeter's plates and are distributed in $0 < \phi < 2\pi$. The ordinate in figure 2b is the distance from the IP, along the depth of the calorimeter. Electrons produce relatively narrow showers, within the EM section of the calorimeter (compare with figure 3).

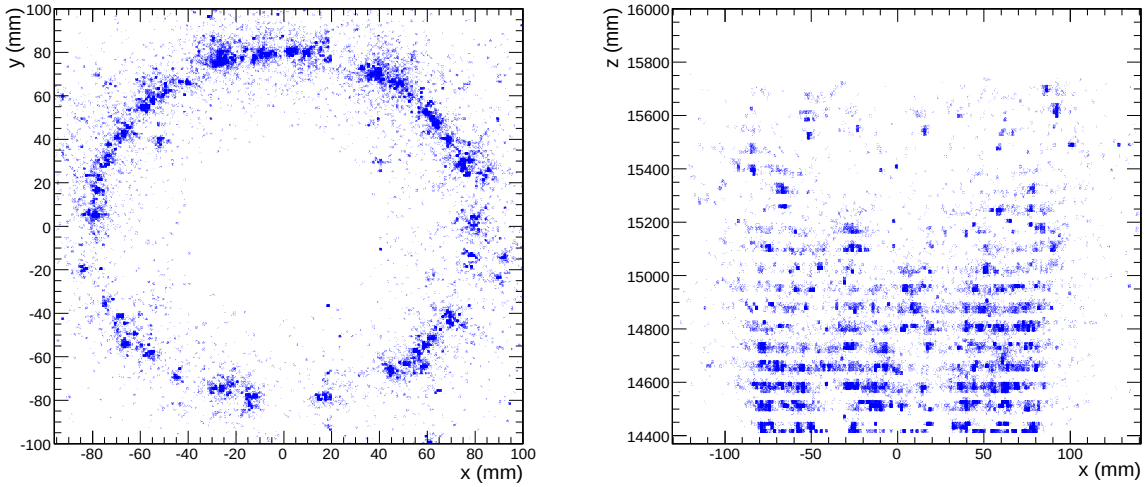

Figure 3: Cherenkov light yield transversal and longitudinal profile, produced by incoming 50GeV pions. The particles enter at the center of the calorimeter's plates and are distributed in $0 < \phi < 2\pi$. The ordinate in 3b is the distance from the IP, along the depth of the calorimeter. Compared to electrons (see figure 2), pions produce wider and more penetrating showers.

For the Cherenkov photon production, a dedicated algorithm has been developed: For charged particles passing through the sensitive material with velocity above the Cherenkov threshold ($\beta_{threshold} = 0.67$ for quartz), the average number of produced Cherenkov photons is calculated. A fraction of the total number of emitted photons is finally collected, depending on the incoming particle direction. The efficiency of light transmission through the light guide is also taken into account.

3.1 Energy Response Linearity

The energy response of the calorimeter has been studied with gammas, electrons and pions of energy 20- 1000 GeV, Figures 4a - 6a, respectively. The gamma and electron shower is found to be contained mainly in the one sector of impact and within the electromagnetic section. The pion shower is seen weekly in neighbouring sectors at the rear of the calorimeter.
For all beams, the calorimeter response is found to be linear in the energy range explored. The average signal amplitude, expressed in units of ADC channels, can be well fitted by the following formula:

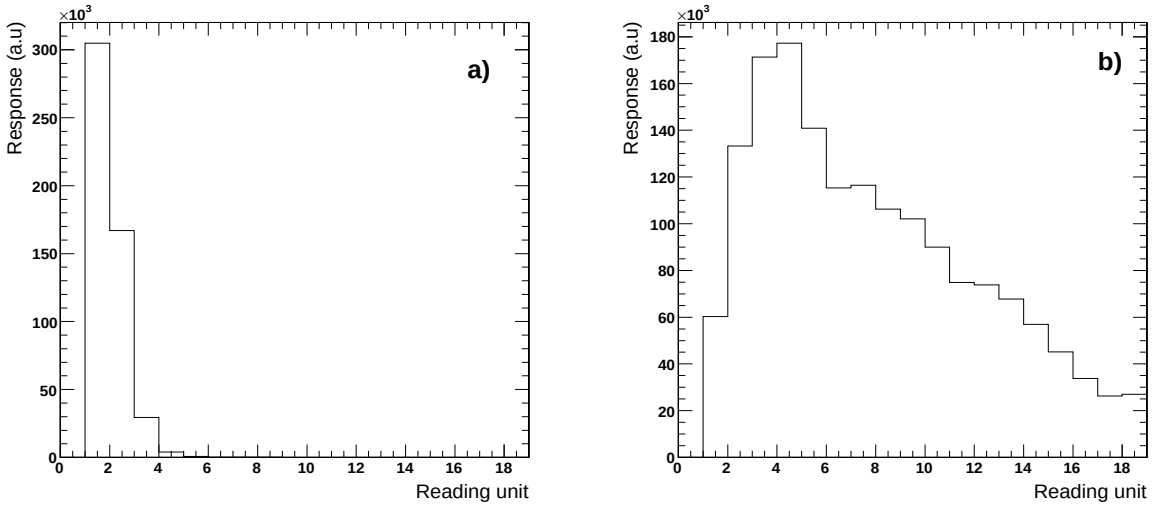

Figure 4: Number of cherenkov photons collected per reading unit a) for incoming 100GeV electrons and b) for incoming 100GeV pions.

$$ADC = a + bE \tag{1}$$

where the energy E is in GeV. The fitted values of the parameters for each configuration are shown in Figures 4a - 6a. The constant term is negative, indicating the threshold behaviour of this type of calorimeter. Only incident particles above a certain energy can produce charged secondaries with velocities above the Cherenkov threshold for a measurable signal.

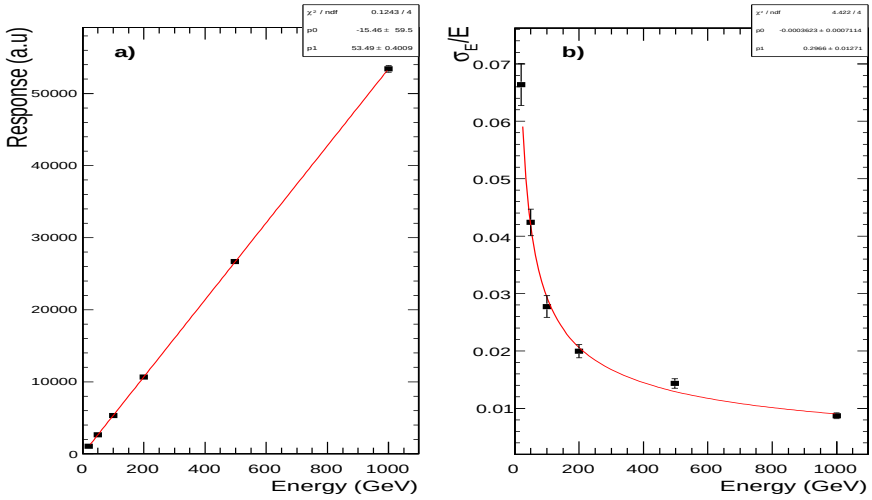

Figure 5: a) Energy linearity and b) resolution of the CASTOR calorimeter fitted by $\frac{\sigma}{E} = P_0 + \frac{P_1}{\sqrt{E}}$ for photons.

3.2 Energy Resolution

The energy resolution for gammas, electrons and pions has been studied in the same energy range. The relative energy resolution of the calorimeter has been obtained by fitting the normalized width of the Gaussian signal amplitudes, σ/E, with respect to the incident beam energy, E (GeV) by the expressions:

$$\frac{\sigma(E)}{E} = P_0 \oplus P_1/\sqrt{E} \oplus P_2/E \tag{2}$$

$$\frac{\sigma(E)}{E} = P_0 + \frac{P_1}{\sqrt{E}} \tag{3}$$

where $\oplus$ indicates summing in quadrature. The fits, employing relation (2), are shown in Figures 4b - 6b for

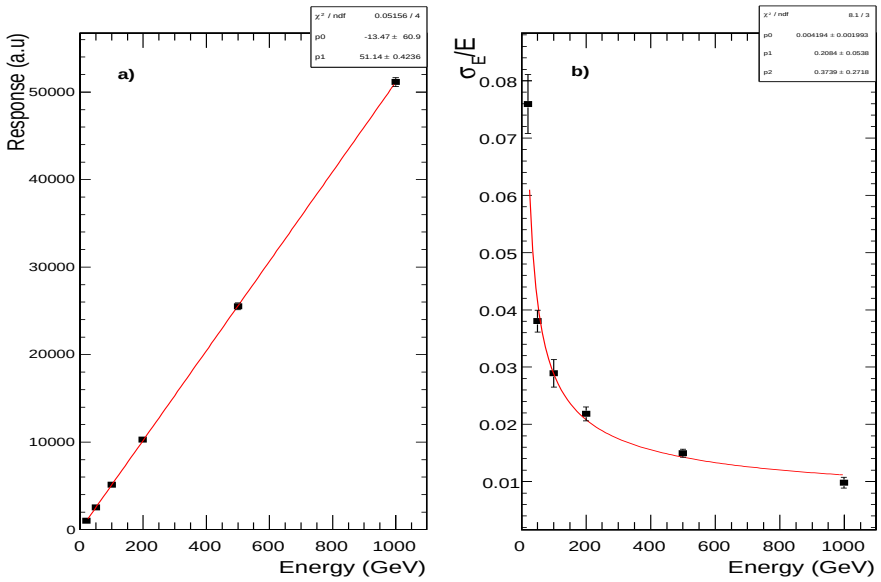

Figure 6: a) Energy linearity and b) resolution of the CASTOR calorimeter fitted by $\frac{\sigma}{E} = P_0 + \frac{P_1}{\sqrt{E}}$ for electrons.

gammas, electrons and pions, respectively. Both expressions describe the data equally well. The results of the fits are shown in Tables 1, 2.

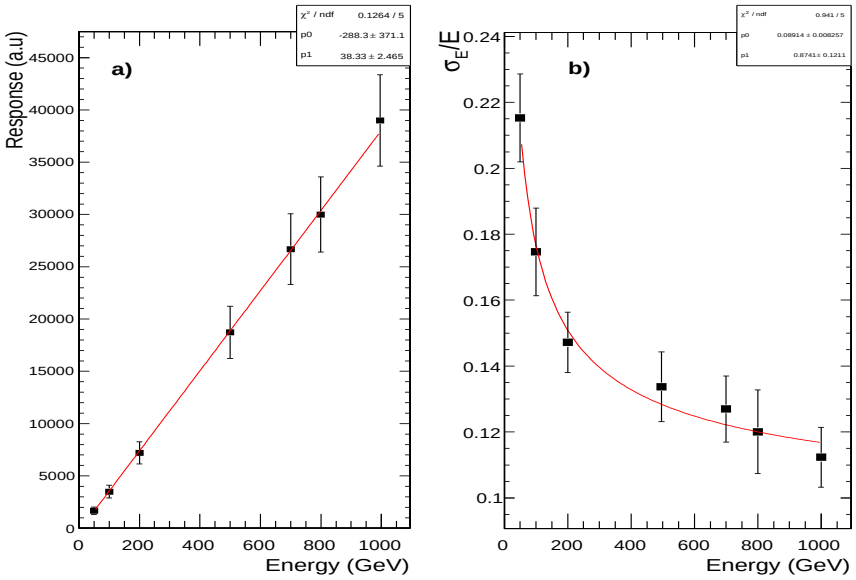

Figure 7: a) Energy linearity and b) resolution of the CASTOR calorimeter fitted by $\frac{\sigma}{E} = P_0 + P_1/\sqrt{E}$ for pions.

3.3 e/π ratio

The response to the electrons over the response to the pions has been calculated for the energy range 50 - 1000 GeV and is shown in Figure 8. The simulated e^-/π ratio is energy dependent for energies below 100 GeV. At higher energies it attains an almost constant value of about 1.41.

4 Comparison with fibers

A similar Monte Carlo simulation was performed for a tungsten/quartz fiber calorimeter [4]. The geometry of this calorimeter had as sampling unit a 3mm tungsten absorber and 2 fiber-planes with filling ratio of 33.5%. The readout unit consisted of 15 sampling pairs. The calorimeter was azimuthally segmented into 8 sectors ($\phi = 45$).

Table 1: Fit parameters.

$\sigma(E)/E = P_0 \oplus P_1/\sqrt{E} \oplus P_2/E$	p_0	p_1	p_2
electrons	(0.007 ± 0.001)	(0.27 ± 0.02)	(0.7 ± 0.3)
γ's	$(-9 \cdot 10^{-10} \pm 0.004)$	(0.29 ± 0.01)	(0.34 ± 0.34)
pions	(0.112 ± 0.006)	(1.3 ± 0.1)	$(6 \cdot 10^{-8} \pm 7)$
$\sigma(E)/E = P_0 + P_1/\sqrt{E}$	p_0	p_1	
electrons	(0.0018 ± 0.0009)	(0.28 ± 0.01)	
γ's	(-0.0003 $\pm$ 0.0007)	(0.30 ± 0.01)	
pions	(0.089 ± 0.008)	(0.87 ± 0.12)	

Table 2: Energy resolution for electrons and pions.

E (GeV)	electrons	γ's	pions
20	$(7.60 \pm 0.52)\%$	$(6.64 \pm 0.36)\%$	
50	$(3.80 \pm 0.20)\%$	$(4.23 \pm 0.23)\%$	$(21.5 \pm 1.3)\%$
100	$(2.90 \pm 0.24)\%$	$(2.77 \pm 0{,}19)\%$	$(17.4 \pm 1.3)\%$
200	$(2.18 \pm 0.12)\%$	$(2.00 \pm 0.12)\%$	$(14.7 \pm 0.9)\%$
500	$(1.50 \pm 0.07)\%$	$(1.43 \pm 0.08)\%$	$(13.3 \pm 1.1)\%$
700			$(12.7 \pm 0.1)\%$
800			$(12.0 \pm 0.1)\%$
1000	$(0.98 \pm 0.09)\%$	$(0.87 \pm 0.05)\%$	$(11.2 \pm 0.9)\%$

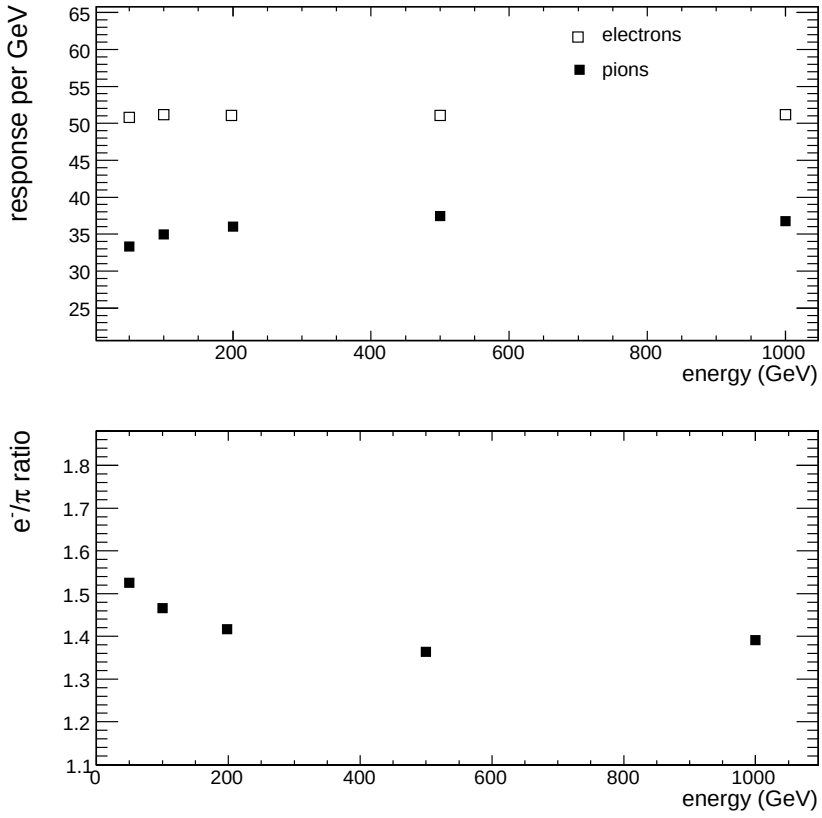

Figure 8: Response per GeV to electrons and pions and the corresponding e^-/π ratio.

The simulated energy resolution was found to be [1]:
$\frac{\sigma(E)}{E} = (0.00 \pm 0.04)\% \oplus \frac{(21.0 \pm 0.3)}{\sqrt{E}}\%$,
$\frac{\sigma(E)}{E} = (6.4 \pm 0.3)\% \oplus \frac{(89. \pm 3.)}{\sqrt{E}}\%$
for electrons and pions, respectively, and the e/π ratio $\simeq 1.25$. These values are in good agreement with the ones

[1] The simulations were performed for various total calorimeter depths. The average value for 200 and 250 layers, corresponding to 9.2 and 11.5 λ_I's were used for comparison.

Table 3: Calculated e^-/π ratio.

E (GeV)	e^-/π ratio
50	1.525
100	1.466
200	1.413
500	1.364
1000	1.391

from the present simulation for a tungsten/quartz plate calorimeter [2)]:
$\frac{\sigma(E)}{E} = (0.57 \pm 0.16)\% \oplus \frac{(29.\pm 1.)}{\sqrt{E}}\%$,
$\frac{\sigma(E)}{E} = (8.9 \pm 0.8)\% \oplus \frac{(87.\pm 12.)}{\sqrt{E}}\%$
for electrons and pions, respectively and e/π ratio = 1.41.

5 Leakage

The "leakage" of the calorimeter was studied with electrons and pions in the energy range 100-1000 GeV. In the case of incoming electrons, the leakage is defined as the ratio of the number of photoelectrons collected in the hadronic reading units to their respective number collected in the electromagnetic section of the detector. For incoming pions, the leakage is defined as the inverted ratio, for $20X_0$ deep EM section, i.e

$$EM - leakage = \frac{\#photoelectrons\ in\ hadronic\ RUs}{\#photoelectrons\ in\ EM\ RUs} \tag{4}$$

$$H - leakage = \frac{\#photoelectrons\ in\ EM\ RUs}{\#photoelectrons\ in\ hadronic\ RUs} \tag{5}$$

The electromagnetic section consists of the first two reading units of the calorimeter ($\sim 20X_0$). However we have also calculated the leakage that corresponds to a total of three electromagnetic reading units.

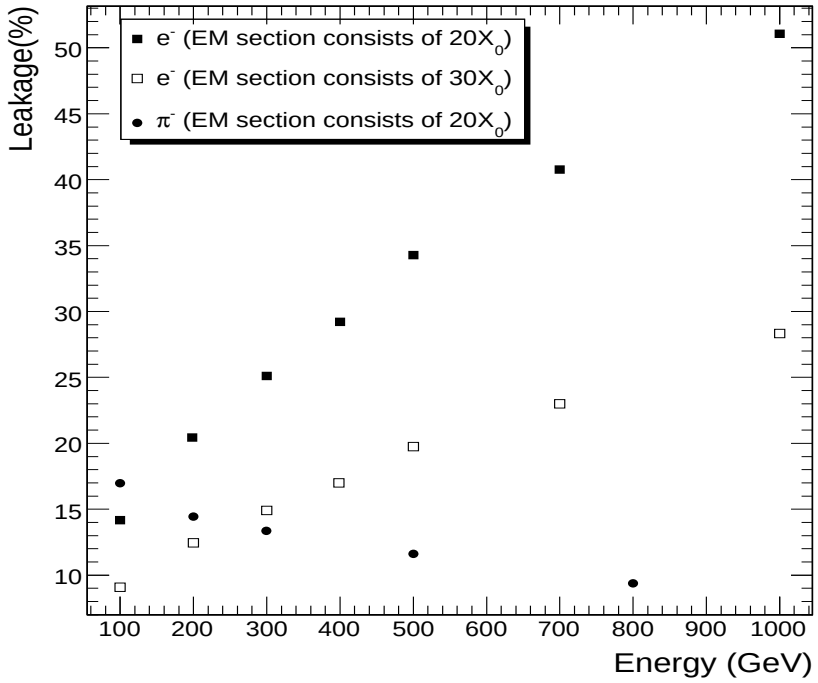

Figure 9: Electromagnetic and hadronic leakage as defined in equations (4), (5)

.

[2)] For the comparison only, the energy resolution was fitted by the expression $\frac{\sigma}{E} = P_0 \oplus P_1/\sqrt{E}$

6 Summary

Some basic characteristics of the CASTOR calorimeter have been studied with Monte Carlo simulations. For the described geometry of the detector, the energy response linearity and resolution for gammas, electrons and pions, as well as the e/π ratio were obtained. The calorimeter exhibits linear response up to the energy of 1000 GeV studied. The energy resolution for gammas and electrons was found to be below 3% for energies above 100 GeV, while for pions it was below 18%.

Acknowledgements

This work is supported in part by the Secretariat for Research of the University of Athens.

References

[1] Castor calorimeter webpage: http://cmsdoc.cern.ch/castor/

[2] A.L.S. Angelis *et al.*, *EPJdirect* C9, 1-18, 2000

[3] A.L.S. Angelis and A.D. Panagiotou, *J.Phys.G23:2069-2080*, 1997;
A.L.S. Angelis et al., Presented at 28th International Symposium on Multiparticle Dynamics, Delphi, Greece, 6-11 Sep 1998; hep-ex/9901038,
A.L.S. Angelis et al., *Nucl.Phys.Proc.Suppl. 97:227-230*, 2001.

[4] G. Mavromanolakis, A. L. S. Angelis, A. D. Panagiotou, *ALICE-INT-2000-20, Internal Note/CAS*, 2000.